

Relativistic jets: an astrophysical laboratory for the Doppler effect

Nadia L. Zakamska

*Department of Physics and Astronomy, Johns Hopkins University,
3400 N. Charles St., Baltimore MD 21218*

Abstract

Special Relativity is one of the most abstract courses in the standard curriculum for physics majors, and therefore practical applications or laboratory exercises are particularly valuable for providing real-world experiences with this subject. This course poses a challenge for lab development because relativistic effects manifest themselves only at speeds close to the speed of light. The laboratory described in this paper constitutes a low-cost, low-barrier exercise suitable for students whose only background is the standard mechanics + electromagnetism sequence. The activity uses research-quality astronomical data on SS433 – a fascinating Galactic X-ray binary consisting of a compact object (a neutron star or a black hole) and a normal star. A pair of moderately relativistic jets moving with $v \sim 0.3c$ in opposite directions emanate from the vicinity of the compact object and are clearly detected in optical and radio observations. Following step-by-step instructions, students develop a full kinematic model of a complex real-world source, use the model to fit the observational data, obtain best-fit parameters, and understand the limitations of the model. The observations are in exquisite agreement with the Doppler effect equations of Special Relativity. The complete lab manual, the dataset and the solutions are available in online supplemental materials; this paper presents the scientific and pedagogical background for the exercise.

I. INTRODUCTION

Special Relativity – a study of time and space in reference frames which are moving at high speed relative to one another – is at the top of the list for the most abstract topics in undergraduate science curriculum. Students are often shocked to discover that Special Relativity is far from being a vague discussion of qualitative properties of space and time and that they are expected to perform actual calculations of energies and trajectories of fast-moving objects, without any real-world experience with such phenomena. As a result, one of the most common questions in the first few lectures of Special Relativity is “What is the relevance and applicability of this material?”.

A typical textbook problem in Special Relativity involves runners or vehicles catching up to one another at a speed approaching the speed of light, hardly the stuff of everyday experiences. An improvement in student engagement can often be achieved in the lectures by emphasizing and discussing the routine applications of Special Relativity in astrophysics and particle physics³³. Even more desirable would be laboratory activities that allow hands-on experiences with relativistic phenomena, but few such labs are available^{7,28}, and because Special Relativity only manifests itself at velocities close to the speed of light lab designs can be severely limited by costs.

In this paper I present a zero-cost laboratory exercise in Special Relativity. The lab uses research-quality data collected over many years by professional scientists to measure the relativistic Doppler effect in a unique astronomical source. The lab can be incorporated into any course on Special Relativity that covers the relativistic Doppler effect. It does not require any background other than the standard freshman sequence of mechanics and electromagnetism. Furthermore, while the full model obtained toward the end of the lab is fairly mathematically complex, it is algebra-based, not calculus-based. As a result, the lab has been successfully used at Johns Hopkins University (JHU) since 2012 in a seven-week mini-course on Special Relativity normally taken in the beginning of the sophomore year.

In Section II, I describe the scientific content of the lab and the standard exercise setup implemented at JHU. As designed, the exercise has minimal pre-requisites and a low barrier for entry, but it can be adapted to higher complexity levels. Therefore, in Section III I discuss learning objectives and presentation of the lab to the students and describe potential advanced enhancements. I conclude in Section IV.

II. SCIENTIFIC CONTENT AND SETUP OF THE SS433 LAB

A. Astrophysical nature of the source

SS433 was discovered in late 1970s as a Galactic source associated with $H\alpha$ and X-ray emission^{30,31}. It is now understood as a binary star in a 13-day orbit⁴, in which a compact object (a black hole or a neutron star) is accreting matter shed by a normal stellar companion. The accretion proceeds at an unusually high rate, possibly in excess of the Eddington threshold, making this source a unique laboratory for studying some of the extreme manifestations of the accretion phenomenon^{2,9}.

Despite many years of study, the nature of the compact object has not yet been unambiguously determined. Such determinations are based on the mass measurement, with neutron stars typically having $M \simeq 1.4M_{\odot}$ and black holes having much greater masses ($M > 5M_{\odot}$), but in this system the dynamical mass estimates which rely on measurements of orbital velocity and on the stellar mass of the normal companion have yielded a wide range of results^{6,13,14}, with a black hole generally preferred, but a neutron star not yet excluded. Part of the problem is that the donor star is difficult to detect and to characterize because the total optical and ultraviolet flux is not only dominated by the accretion onto the compact source, but is also affected by strong interstellar absorption¹². Based on the available observations and spectral modeling, the donor star is tentatively classified as an evolved A-type star¹¹.

Jets – rapidly moving narrow streams of matter, ejected along the polar axis of the accretion disk – are a common outcome of accretion, found in a wide range of astrophysical systems. The compact object in SS433 launches mildly relativistic $v \simeq 0.3c$ jets which produce optical¹, X-ray³² and possibly gamma-ray emission lines¹⁶ (though this detection is disputed¹⁰), which correspond to known electronic transitions within atoms or ions of normal chemical elements or to their nuclear transitions. These observations demonstrate that the jet in SS433 has a significant and possibly a dominant²⁴ baryonic component, one of only two such jets known⁵. All other jets launched by compact objects produce featureless spectra, and one of the fascinating mysteries of astrophysics is whether their energy flux is dominated by baryons, electron-positron pairs or other forms.

The lab is administered to the students during a section led by graduate teaching assis-

tants (who are not necessarily experts in astronomy) in the form of a PDF document that contains instructions and questions to be answered, and an electronic file with SS433 data. These materials, along with the lab solutions, are provided as online supplements to this publication. The lab begins with links to popular science webpages²⁵ which show cartoon descriptions of the salient components of SS433 described above. The lab instructions then state the goals of the lab: (1) students will not collect any new data, but they will analyze data on the jets of SS433 collected by professional astronomers over many years; (2) students will follow step-by-step instructions to construct a kinematic model of the jets and use the model to represent real data; (3) as nature rarely presents itself in the form of idealized problems, students will practice breaking a complex astrophysical situation into manageable pieces, which is usually the necessary first step in any scientific research. Students discuss some of the exercises with their teaching assistant and finish the lab at home, as they would a regular homework. The final result of the lab is a graded lab report that contains answers to the questions posed in the lab instructions and the presentation and the results of the kinematic model.

B. Data to be modeled

Although multiple different emission features trace the kinematics of the jet, in this lab we model specifically the time evolution of the Balmer lines of atomic hydrogen which constitute the most complete kinematic dataset^{1,8,20,21}. As part of the lab instructions, the students are given a two-page introduction into the physics of the hydrogen emission lines which does not require any prior knowledge of quantum mechanics. At optical wavelengths, hydrogen – the dominant chemical element in the universe and in the jet of SS433 – emits most of available energy in emission lines whose laboratory wavelengths are set by the laws of quantum mechanics and are provided to the students. Students can then be asked several qualitative questions to test understanding of this material.

Students then consider a blob of hydrogen moving with velocity \mathbf{v} in space and derive (or reproduce the derivation given in their special relativity class) the Doppler effect formula in the form

$$\lambda = \lambda' \gamma (1 - \mathbf{v} \cdot \mathbf{n}/c). \quad (1)$$

Here λ' is the wavelength of light in the emitter's frame, λ is the wavelength seen by the

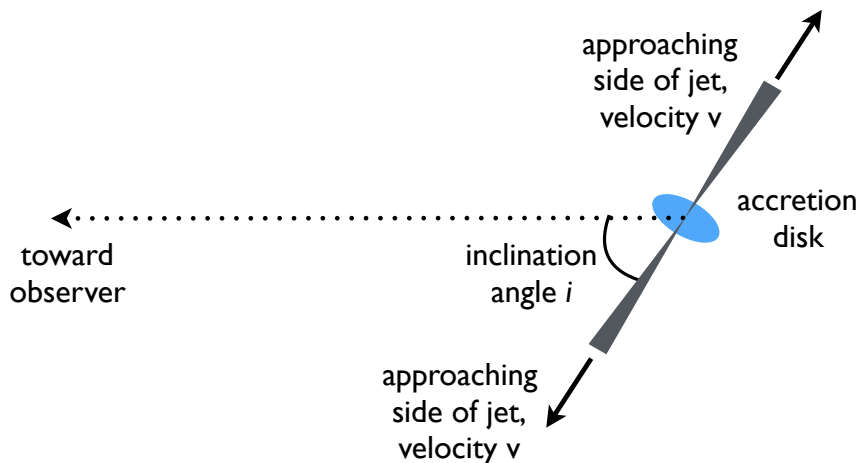


FIG. 1. Assuming that the jet is intrinsically symmetric, only two parameters – its velocity v and its inclination to the observer i – are necessary to describe the observed wavelengths of the emission features originating in the receding and in the approaching parts of the jet.

observer on Earth, $\gamma \equiv 1/\sqrt{1 - v^2/c^2}$ is the Lorentz factor of the blob, c is the speed of light, and \mathbf{n} is the unit vector in the observer's frame directed from the emitter to the observer.

Armed by this equation, the students proceed to analyze published spectra of SS433 taken on three consecutive nights²¹ which are reproduced in the lab handout. Each spectrum contains three prominent emission lines. The central emission line stays at the same wavelength in all three frames – this is the $H\alpha$ emission line produced by the accretion disk. In addition, in each spectrum there are two emission lines flanking the main line. The students are then asked to measure the central wavelengths of the flanking emission lines – this is usually done with a ruler off of the paper print-out of the lab instructions – and to estimate the uncertainty of their measurement. At this point they confront the reality that the lines have an irregular shape, so the centroid can only be determined to no better than 10\AA , which is comparable to the typical uncertainty of the ruler.

Taking one of the spectra, the students obtain measurements of the apparent wavelength of flanking lines λ_1 and λ_2 . They are then asked to consider a symmetric jet inclined at some angle i to the observer's line of sight, with one side approaching the observer and one side receding from the observer (Figure 1). Applying equation (1) to this model, we obtain

two equations for the two flanking lines:

$$\lambda_1 = \lambda' \gamma (1 - v \cos i/c); \quad (2)$$

$$\lambda_2 = \lambda' \gamma (1 + v \cos i/c), \quad (3)$$

where the proper wavelength of the H α emission $\lambda' = 6563\text{\AA}$ is the same for both lines. With two measurements (λ_1 and λ_2) this system of equations can be solved for the two unknowns in this instantaneous snapshot of the system – the jet’s inclination angle and its velocity. Adding the two equations, we obtain $\gamma = (\lambda_1 + \lambda_2)/2\lambda'$, which gives the jet’s velocity. My own calculation at this step yields $v = 0.262c$, which is within 5% of the best measurements of the SS433 jet velocity available in the scientific literature, quite remarkable for a “ruler off paper graph” measurement approach! The students can then be asked further questions to test their understanding of the basic jet model – for example, whether this calculation would be possible without the assumption of the intrinsic symmetry of the jet.

C. Full kinematic model of the precessing jet of SS433

As if having jets moving with relativistic velocities was not exotic enough, it turns out that the jets are not stationary in space, but are precessing. To understand the three-dimensional geometry of the system in the presence of precession, the students are given a link to the radio snapshots of the jet assembled into a time-lapse movie²⁶. The jet is somewhat clumpy, so rather than smooth streams the movie shows individual blobs propagating away from the compact object on trajectories that are slowly rotating in the plane of the sky as the jet precesses. On larger scales, students can see the remnants of the old precession cycles forming a “corkscrew” pattern³.

It is precisely because of the precession that the flanking emission lines produced by the jet do not stay at the same wavelengths in the three example spectra²¹ analyzed in Section II B. Because the orientation of the jet changes as a function of time, the magnitude of the Doppler effect changes as well, and so does the observed wavelength of H α . The next step of the lab is to develop the complete kinematic model to reproduce the time-varying H α observations and to measure the precession period^{1,8,20}. A historical account of the discovery of the system, of precession modeling and of example spectra is available in a “Scientific American” article suitable for sophomores¹⁸, but it does contain solutions to some of the

lab exercises, and therefore we do not distribute this article as part of our default JHU lab setup. It may be useful for instructors and teaching assistants in class preparation.

A collection of H α centroid measurements taken over 14 years was kindly provided B. Margon and is given to students in a machine-readable format as part of this lab. The file tabulates the Julian Date of the observation (measured in days) and $z \equiv (\lambda - \lambda')/\lambda'$ for each of the two sides of the jet. The lab uses the same astronomical definition for redshift z as the standard notation used in cosmological observations; negative values are allowed and imply a blueshift.

The students are asked to make the following assumptions: (1) The absolute value of the velocity of the jet always stays the same on both sides, even though the orientation of the jet changes; (2) The two sides of the jet are always moving in opposite directions; (3) The precession sweeps a conical surface with a constant angular frequency. With these assumptions, the only term in equation (1) which changes as a function of time is $\mathbf{v} \cdot \mathbf{n}$, and that only because the angle between the two vectors (rather than their absolute values) varies due to precession.

The students are given the cartoon shown in Figure 2 and are then asked how many model parameters are necessary to describe the full precessing model. There are five: the material in the jet moves with velocity v ; the cone swept by the precessing jet is completely defined by the inclination of its axis to the line of sight I and its opening angle θ ; and the timing of the precession is specified by the angular speed of precession ω , with t_0 being the time when the jet passes closest to the line of sight.

With this notation, the most mathematically difficult aspect of the lab is to connect the five model parameters with the $z(t)$ values tabulated in the data file⁸. The instantaneous inclination of the jet to the line-of-sight i used in the previous section is a function of the cone's geometry (specified by I and θ) and depends on when during the precession cycle the jet is observed, so it is a function of all parameters except velocity. The derivation uses vectors and trigonometry and is given in the lab solutions (provided to the graduate teaching assistants ahead of the lab).

Specifically, we introduce a system of Cartesian coordinates with the z -axis along the symmetry axis of the cone and the observer in the $x - z$ plane. Then the unit vector from the emitter to the observer is $\mathbf{n} = \mathbf{e}_z \cos I + \mathbf{e}_x \sin I$. In the same coordinate system, the velocity vector of the material of the approaching side of the jet is $\mathbf{v} =$

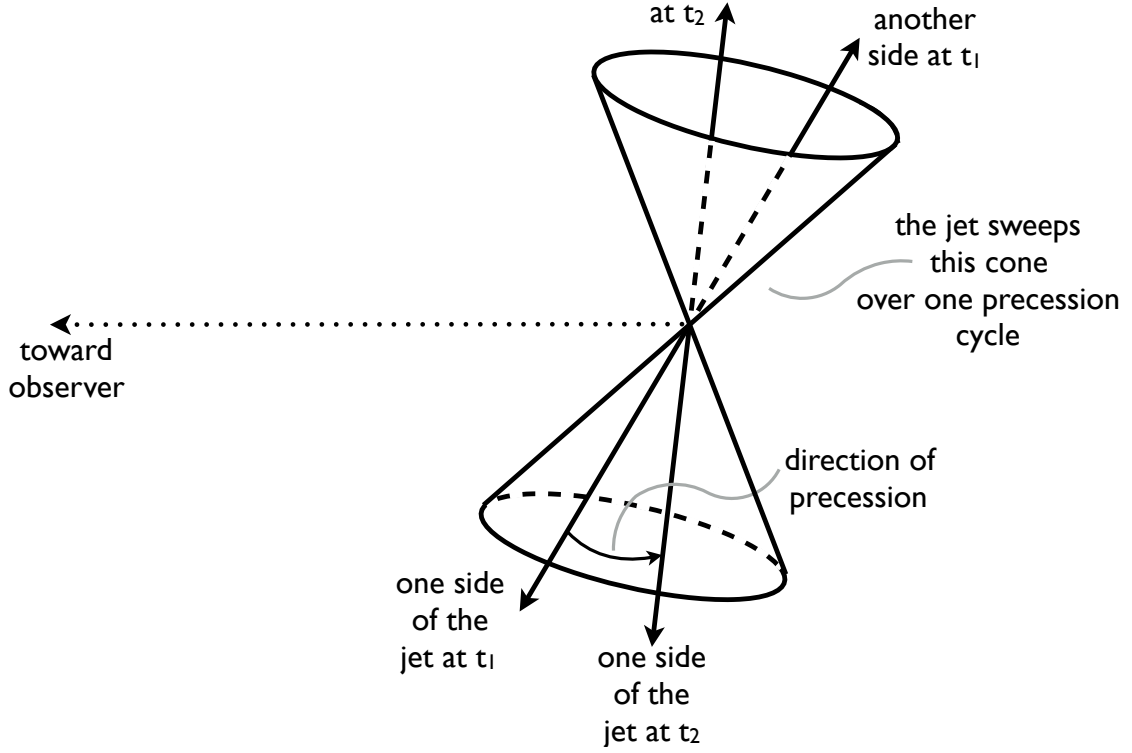


FIG. 2. Schematic of the complete precession model for SS433. Over one precession period, the jet sweeps a conical surface, thereby changing the orientation of the jet's movement relative to the line of sight and the magnitude of the Doppler effect. As a result, the emission lines produced by the jet appear at different observed wavelengths during different phases of the precession cycle.

$v(\mathbf{e}_z \cos \theta + \mathbf{e}_x \sin \theta \cos(\omega t - \omega t_0) + \mathbf{e}_y \sin \theta \sin(\omega t - \omega t_0))$. Combining these equations with equation (1) and with the definition of redshift, we find that one side of the jet would be observed with

$$z(t) = \gamma \left(1 - \frac{v}{c} \sin I \sin \theta \cos(\omega t - \omega t_0) - \frac{v}{c} \cos I \cos \theta \right) - 1; \quad (4)$$

and for the other side of the jet we need to replace v with $-v$.

D. Results of the modeling

A major skill now required of many advanced physics students is that of plotting data and models using modern scientific software, and of fitting models to the data. Depending on the software availability and programming level of the students, modeling of the data with the complete kinematic model in equation (4) can be performed on a variety of levels

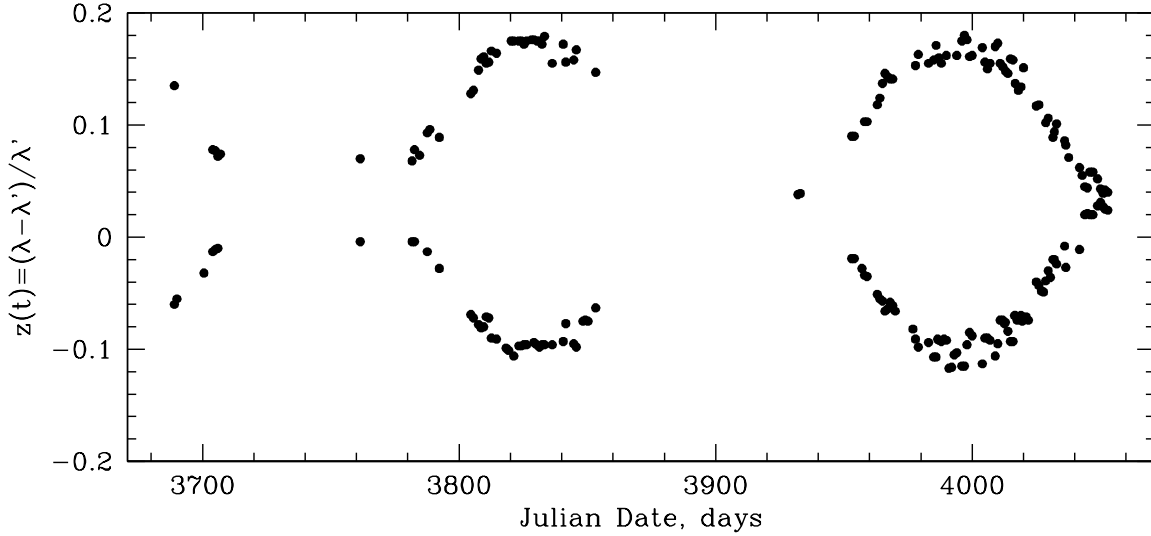


FIG. 3. The first two precession cycles from the SS433 data file. The periodic behavior is clearly seen, and so are the “crossing points” where both sides of the jets show the same Doppler effect, e.g., at $t = 4050$ days.

of complexity. At JHU, the lab on SS433 is among the first steps in developing these skills. No prior computing knowledge is assumed, and we use `Mathematica` to represent the data and the models as a site license is available for all students.

As part of the lab, the students are given a one-page introduction on some of the basic commands in `Mathematica` that allow them to display $z(t)$ entries from the SS433 data file. Unless they have technical skills to read in the entire file, they are asked to select a dozen or two entries spanning roughly a year and sampling as uniformly as possible. Having plotted these values, they should be able to see some interesting features in the time dependence of the jet components (Figure 3) and they can be asked a series of qualitative questions to explain these features.

For example, the $z(t)$ curves from the two sides of the jet cross at some moments (e.g., at $t = 4050$ days in Figure 3), which means that at these times the two emission lines from the different sides of the jet blend into one. The students are asked to consider why this might occur in the precession model. These incidents correspond to moments when the jets are propagating exactly in the plane of the sky, without any velocity component along the line of sight to the observer. Interestingly, this happens at a positive value of z for both sides,

which is a manifestation of the transverse Doppler effect with $\lambda = \gamma\lambda'$, a purely relativistic phenomenon not present in the Doppler effect for sound waves in classical mechanics. The value of z during these crossing moments ($\simeq 0.0363$) independently constrains the velocity of the jet.

The final exercise for the lab is to guess as many parameters of the full kinematic model as possible from the shape of the curve and to use these parameters to show the model curve from equation (4) together with the data points. In an ideal case, students achieve a good agreement between their model and the data after just a few tries for the model parameters. At the sophomore level, no formal fitting (in the sense of χ^2 minimization or global minimum search in the parameter space) is required, and in fact guessing the parameters to crudely reproduce the curves is preferred in order for students to develop a physical intuition for which features of the dataset constrain the precession model parameters.

For example, in analyzing the data in Figure 3, v can be fixed to the previously calculated value from an instantaneous spectral measurement, $v = 0.262c$. Furthermore, t_0 is the time when the jet makes the smallest angle to the line of sight, so it should correspond to the maximum blueshift of one side of the jet and the maximum redshift of the other side, so we can estimate $t_0 = 3990$ days from the second peak in Figure 3. The angular frequency of precession ω is equal to $2\pi/P$, where P , the period, is the time between two peaks, $\simeq 165$ days (the published value is 162.375 days⁸). The opening angle θ and the inclination angle of the cone axis I can be guessed by looking at the difference between the maxima and minima of each of the $z(t)$ curves. In particular, the combination of $I - \theta$ is found from the maxima and minima using the same method as in Section II B, as during these epochs the blue-shifted side of the jet forms an angle $I - \theta$ to the line of sight.

After the $z(t)$ curves “cross”, the jets continue precessing and they change orientation: the side that was previously approaching recedes for some fraction of the period, and vice versa. In the first two precession cycles I chose for Figure 3, the observations do not sample well this part of the cycle, which constrains the combination $I + \theta$ (other parts of the dataset offer better phase coverage). If this happens, the student can show a variety of models that fit the data instead of aiming for the best-fitting one. In Figure 4, the model with three guessed parameters and two taken from the formal fit⁸ is shown for comparison with data, to demonstrate a typical accuracy that can be achieved by the kinematic model without a formal χ^2 minimization.

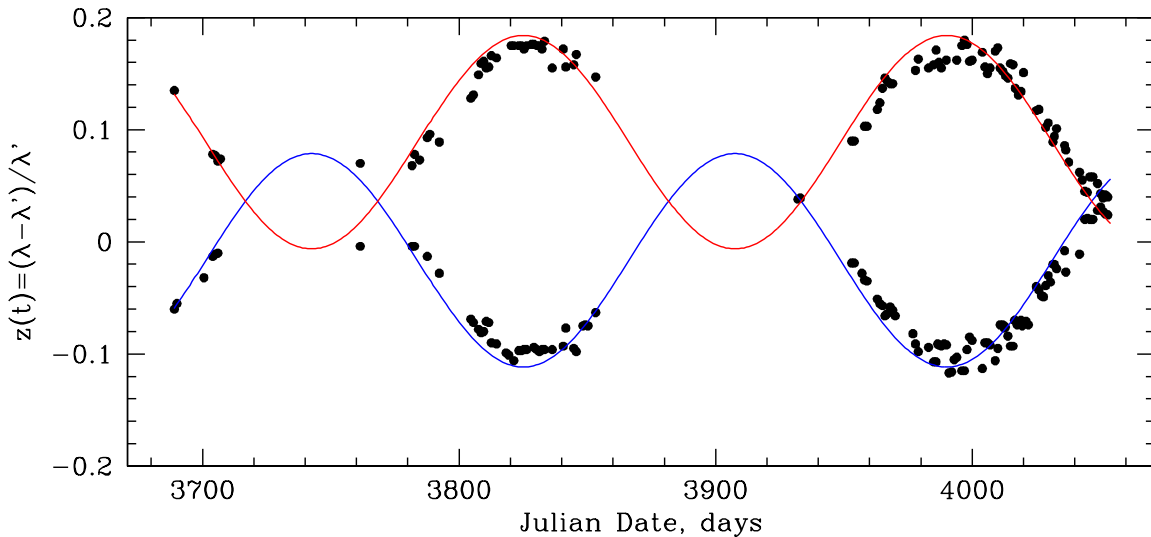


FIG. 4. The same dataset as above, with the guessed model overlaid, with $t_0 = 3990$ days, $P = 165$ days, $v = 0.262c$ from measurements in Section II B. The inclination of the cone’s axis is set to $I = 78$ degrees and the opening angle to $\theta = 21$ degrees⁸, but students should try several different values to develop a sense for their impact on the model.

The kinematic model fits the Doppler shift data to better than $|\Delta z| < 0.02$ over decades of observations, though there are systematic residuals some of which are understood and some that are not^{8,15}. To be able to derive the velocity of the jet to within a few per cent with just one observation in Section II B and to be able to guess the parameters of the kinematic model to better than 10% in Section II C is quite unique in astrophysics. It can be emphasized to students that the model does not offer a perfect description of the data both due to measurement errors of the emission line centroids and because of astrophysical complications; yet the value of the kinematic model is in being able to explain the dominant behavior of the system over many decades.

While the precession appears stable over the timescale of the observations, the physical mechanism of the precession is poorly understood. It is thought that the jet propagates exactly along the polar axis of the accretion disk, so the precession of the jet must reflect the precession of the accretion disk. This was indeed found to be the case – the accretion disk’s precession is inferred from brightness monitoring of SS433 and has the same period as the jet¹⁹. The disk in turn may be precessing because it suffers from warping induced by

radiation pressure¹⁷. But because the jet must be launched from the vicinity of the compact source, communicating the precession from the outer parts of the accretion disk to the jet is difficult, and therefore the presence of jet precession may be tied with the unusually high rate of accretion in SS433². The questions about the physical origin of the precession rarely, if ever, come up in the course of the lab. When they do, it is laudable that students can appreciate the difference between a kinematic model and its physical origin and they can be encouraged to explore the scientific references on this topic.

III. LEARNING OBJECTIVES AND CLASS PREPARATION

The default lab instructions as administered at JHU and solutions are available from the author upon request. Depending on the level of the class, the lab can be scaled up or down in difficulty. In this section I build on feedback from students and graduate teaching assistants to provide suggestions on moderating the difficulty level of the lab.

The learning goals of laboratory exercises in the physics sequence can be roughly grouped into (1) designing and building the experiment; (2) conducting, recording and presenting measurements and their errors; (3) analyzing and modeling the measurements; and (4) communicating the results. By comparison to many standard laboratory exercises in classical mechanics, this lab utilizes significantly more complex modeling while de-emphasizing some of the other aspects (e.g., data collection). Nonetheless, the default lab includes questions that address learning goals across the entire range. For example, while a formal treatment of uncertainties is not expected, the students are asked qualitative questions about the uncertainty of the wavelength measurements that they are analyzing.

It is not expected that the lab in its default form will be completed at the section led by the graduate teaching assistant. It is realistic to get through Sections II A and II B during the section, leaving Sections II C and II D as a home assignment. It is desirable to warn students about a significant individual work component to the lab report, especially if they are accustomed to being able to complete their lab reports during the lab time. The lab reports are then graded by teaching assistants as a regular homework.

Although the introductory material in Section II A is presented to students in a publicly accessible way rather than through scientific publications, students still find the amount of introductory material to be extensive. Some of this material can be eliminated – for example,

it is not necessary to include an introduction to the quantum-mechanical transitions inside the hydrogen atom; it would be sufficient to simply supply the rest wavelength of the $H\alpha$ transition. Furthermore, the data file containing $z(t)$ can be re-cast by the instructor into a file with $\lambda(t)$ values, thereby eliminating the need to introduce redshift. I choose to maintain this information in the default lab setup because I have seen evidence of excellent retention of this material by students.

The most mathematically challenging part of the lab is the development of the full kinematic model as a function of the model parameters. If the students cannot develop the correct model as a function of model parameters, they might not be able to achieve a good fit. This is a risk we are willing to take in the default setup administered at JHU to encourage the students to push their applied math skills. The model in equation (4) has a certain tolerance for mathematical sloppiness, so students often achieve good fitting results even after somewhat flawed derivations. To avoid this mathematical bottleneck and to enable the students to experiment more easily with comparisons between the model and the dataset, the instructors may decide to prioritize the derivation of equation (4) by the teaching assistants during the section time, or even to include the derivation into the lab hand-out.

It should be made clear to graduate teaching assistants that a best-fit model is not desired, and it is preferable if students successfully guess a reasonable fit either by analyzing the dependence of the model on each parameter via plotting experiments or by estimating the parameters from the extrema of the data as is done in this paper. However, if an increase in difficulty level is desired for a more advanced class, then expanding the lab to include a formal search for best-fit parameters is a possible next step.

Finally, the default lab setup includes several extra-credit questions. One problem asks why it is possible to ignore the binary motion (an order-of-magnitude calculation shows that it is much smaller than the velocity of the jet). Another asks about the internal velocities necessary to explain the observed width of the emission lines (a couple of thousand km/s) and about the corresponding temperature ($T \sim 10^9$ K, though in practice the motions within the jet are likely non-thermal^{22,23}). The last one asks students to derive the apparent proper motion of an object moving with relativistic velocities at an arbitrary angle to the line of sight (which can result in an apparent superluminal motion observed in some astronomical sources, though not in SS433²⁷). These questions are more advanced and can be taken out of the lab without any loss to the primary material.

IV. CONCLUSIONS

SS433 is a fascinating astrophysical object which has attracted attention of many scientists in the ~ 40 years since its discovery. The mildly relativistic jets launched by a compact star move at $\sim 30\%$ of the speed of light and provide an excellent illustration of the effects of special relativity. In this paper, I present a suite of laboratory exercises based on research-quality data on SS433 which can be adapted to almost any level of study of special relativity. The lab has zero equipment costs and can be administered by graduate teaching assistants without in-depth astronomy background, yet it allows students to practice and advance some of the standard laboratory skills in an area of physics where laboratory experiences are hard to come by.

My subsequent communications with some of the students who performed the lab exercises revealed excellent retention of material, with one student commenting that the lab “certainly shows where special relativity is relevant in modern areas of research”. This anecdotal experience is in line with many studies which demonstrate that exposure to research-quality data and participation in research greatly improve student engagement²⁹. SS433 offers an excellent opportunity – whether as a lab, as a homework exercise, or as an in-lecture illustration – to engage early-stage physics students with exciting research topics in modern science.

ACKNOWLEDGMENTS

The author gratefully acknowledges Bruce Margon for discussions, for providing the dataset used in this lab, and for his permission to disseminate this dataset in support of lab exercises on SS433. The author further thanks Edwin Chan, Stephen Eikenberry, Holland Ford, Wenzer Qin, Steven Wonnell and the two anonymous referees for useful conversations.

-
- ¹ G. O. Abell and B. Margon. A kinematic model for SS433. *Nature (London)*, 279:701–703, June 1979.
- ² M. C. Begelman, A. R. King, and J. E. Pringle. The nature of SS433 and the ultraluminous X-ray sources. *MNRAS*, 370:399–404, July 2006.
- ³ K. M. Blundell and M. G. Bowler. Symmetry in the Changing Jets of SS 433 and Its True Distance from Us. *ApJL*, 616:L159–L162, Dec. 2004.
- ⁴ D. Crampton, A. P. Cowley, and J. B. Hutchings. The probable binary nature of SS 433. *ApJL*, 235:L131–L135, Feb. 1980.
- ⁵ M. Díaz Trigo, J. C. A. Miller-Jones, S. Migliari, J. W. Broderick, and T. Tzioumis. Baryons in the relativistic jets of the stellar-mass black-hole candidate 4U1630-47. *Nature (London)*, 504:260–262, Dec. 2013.
- ⁶ S. D’Odorico, T. Oosterloo, T. Zwitter, and M. Calvani. Evidence that the compact object in SS433 is a neutron star and not a black hole. *Nature (London)*, 353:329–331, Sept. 1991.
- ⁷ J. Dryzek, D. Singleton, T. Suzuki, and R. Yu. An undergraduate experiment to test relativistic kinematics using in flight positron annihilation. *Am. J. Phys*, 74:49, Jan. 2006.
- ⁸ S. S. Eikenberry, P. B. Cameron, B. W. Fierce, D. M. Kull, D. H. Dror, J. R. Houck, and B. Margon. Twenty Years of Timing SS 433. *Astrophys. J.*, 561:1027–1033, Nov. 2001.
- ⁹ S. Fabrika. The jets and supercritical accretion disk in SS433. *Astrophysics and Space Physics Reviews*, 12:1–152, 2004.
- ¹⁰ R. Gelderman and M. Whittle. An optical study of compact steep-spectrum radio sources. 1: The spectroscopic data. *ApJS*, 91:491–505, Apr. 1994.
- ¹¹ D. R. Gies, W. Huang, and M. V. McSwain. The Spectrum of the Mass Donor Star in SS 433. *ApJL*, 578:L67–L70, Oct. 2002.
- ¹² D. R. Gies, M. V. McSwain, R. L. Riddle, Z. Wang, P. J. Wiita, and D. W. Wingert. The Spectral Components of SS 433. *Astrophys. J.*, 566:1069–1083, Feb. 2002.
- ¹³ V. Goranskij. Photometric Mass Estimate for the Compact Component of SS 433: And Yet It Is a Neutron Star. *Peremennye Zvezdy*, 31, Oct. 2011.
- ¹⁴ T. C. Hillwig, D. R. Gies, W. Huang, M. V. McSwain, M. A. Stark, A. van der Meer, and L. Kaper. Identification of the Mass Donor Star’s Spectrum in SS 433. *Astrophys. J.*, 615:422–

- 431, Nov. 2004.
- ¹⁵ J. I. Katz, S. F. Anderson, S. A. Grandi, and B. Margon. Nodding motions of accretion rings and disks - A short-term period in SS 433. *Astrophys. J.*, 260:780–793, Sept. 1982.
- ¹⁶ R. C. Lamb, J. C. Ling, W. A. Mahoney, G. R. Riegler, W. A. Wheaton, and A. S. Jacobson. Gamma-ray line emission from SS433. *Nature (London)*, 305:37–39, Sept. 1983.
- ¹⁷ P. R. Maloney, M. C. Begelman, and J. E. Pringle. Radiation-driven Warping: The Origin of WARPS and Precession in Accretion Disks. *Astrophys. J.*, 472:582, Nov. 1996.
- ¹⁸ B. Margon. The bizarre spectrum of SS 433. *Scientific American*, 243:54–65, Oct. 1980.
- ¹⁹ B. Margon. Observations of SS 433. *ARA& A*, 22:507–536, 1984.
- ²⁰ B. Margon and S. F. Anderson. Ten years of SS 433 kinematics. *Astrophys. J.*, 347:448–454, Dec. 1989.
- ²¹ B. Margon, H. C. Ford, J. I. Katz, K. B. Kwitter, R. K. Ulrich, R. P. S. Stone, and A. Klemola. The bizarre spectrum of SS 433. *ApJL*, 230:L41–L45, May 1979.
- ²² H. L. Marshall, C. R. Canizares, T. Hillwig, A. Mioduszewski, M. Rupen, N. S. Schulz, M. Nowak, and S. Heinz. Multiwavelength Observations of the SS 433 Jets. *Astrophys. J.*, 775:75, Sept. 2013.
- ²³ H. L. Marshall, C. R. Canizares, and N. S. Schulz. The High-Resolution X-Ray Spectrum of SS 433 Using the Chandra HETGS. *Astrophys. J.*, 564:941–952, Jan. 2002.
- ²⁴ S. Migliari, R. Fender, and M. Méndez. Iron Emission Lines from Extended X-ray Jets in SS 433: Reheating of Atomic Nuclei. *Science*, 297:1673–1676, Sept. 2002.
- ²⁵ <http://www.aoc.nrao.edu/~mrupen/XRT/SS433/ss433.shtml>.
- ²⁶ <http://www.aoc.nrao.edu/~mrupen/XRT/SS433/ss433jimovie.gif>.
- ²⁷ https://en.wikipedia.org/wiki/Superluminal_motion.
- ²⁸ G. Pegna. An extraordinary tabletop speed of light apparatus. *Am. J. Phys.*, 85:712, 2017.
- ²⁹ S. H. Russell, M. P. Hancock, and J. McCullough. Benefits of undergraduate research experiences. *Science*, 316:548–549, Oct. 2007.
- ³⁰ F. D. Seward, C. G. Page, M. J. L. Turner, and K. A. Pounds. X-ray sources in the Aquila-Serpens-Scutum region. *MNRAS*, 175:39P–46P, May 1976.
- ³¹ C. B. Stephenson and N. Sanduleak. New H-alpha emission stars in the Milky Way. *ApJS*, 33:459–469, Apr. 1977.
- ³² M. G. Watson, G. C. Stewart, A. R. King, and W. Brinkmann. Doppler-shifted X-ray line

emission from SS433. *MNRAS*, 222:261–271, Sept. 1986.

³³ N. L. Zakamska. Theory of Special Relativity. *ArXiv preprint 1511.02121*, Nov. 2015.